

**Evaluating multiple sensors for mapping cropped area of smallholder  
farms in the eastern Indo-Gangetic Plains**

**by  
Harrison W. Smith**

A thesis submitted in partial fulfillment  
of the requirements for the degree of  
Master of Science  
(Environment and Sustainability)  
in the University of Michigan  
April 2019

Faculty Advisors:  
Assistant Professor Meha Jain, Chair  
Associate Research Scientist Kathleen Bergen



## **Abstract**

Accurate, fine-scale agricultural statistics are critical for understanding trends in crop production throughout the world. In many areas of the world, however, on-the-ground crop area estimates may be difficult to acquire or are only present at state or national scales. In these areas, remote sensing can offer a cost-effective alternative for gathering fine-scale agricultural statistics. Many methods exist for mapping cropped area using remote sensing, but the majority of these are done using moderate-to-coarse spatial resolution sensors such as MODIS or Landsat. Though often finer in scale than state-level data, these sensors may not accurately estimate cropped area in smallholder systems, where a typical agricultural plot can be smaller than a single image pixel. The purpose of this study was to examine the tradeoffs of using four different sensors—MODIS, Landsat 8, Sentinel-2, and PlanetScope—for mapping cropped area in the eastern Indo-Gangetic Plains (IGP) region of India. We used NDVI time series imagery from each sensor to map cropped area for the 2017-2018 winter growing season, and assessed accuracy using classified maps created using random forest classification. We compared each sensor in terms of accuracy, data availability, and ease of use. We find that Sentinel-2 and PlanetScope both show increased accuracies compared to more commonly used sensors such as MODIS and Landsat 8. This indicates that coarse and even moderate resolution sensors, such as MODIS and Landsat 8, may not be sufficient for mapping fine-scale cropped area in smallholder systems. Our results highlight the importance of appropriate sensor selection when mapping cropped area in smallholder systems.

## **Acknowledgments**

I would like to thank to my thesis advisor Dr. Meha Jain, without whom this thesis would not have been possible. I would also like to thank Dr. Preeti Rao for the guidance and advice she contributed to this project, as well as the other members of the Jain lab. It has been a privilege to work with such an amazing group of dedicated people, and I have learned so much from you all. I also want to thank Dr. Kathleen Bergen for serving as my thesis committee member and for her insightful comments. Finally, to my family and my partner Stephanie, thank you for your constant encouragement and support throughout this process.

## Table of Contents

<b>Abstract</b> .....	<b>i</b>
<b>Acknowledgments</b> .....	<b>ii</b>
<b>List of Figures</b> .....	<b>iv</b>
<b>List of Tables</b> .....	<b>v</b>
<b>1. Introduction</b> .....	<b>1</b>
1.1 Background .....	1
1.2 Study Area .....	3
<b>2. Methods</b> .....	<b>5</b>
2.1 Data acquisition and preprocessing .....	5
2.2 Phenology based cropped area classification algorithm .....	5
2.3 Validation using random forest classification.....	7
<b>3. Results</b> .....	<b>9</b>
3.1 Comparison of methods for separating cropped and fallow fields .....	9
3.2 Cropped area map accuracy assessment .....	9
3.3 Evaluating sensors in terms of three criteria.....	9
<b>4. Discussion</b> .....	<b>11</b>
4.1 The role of sensor resolution in cropped area mapping in the eastern IGP .....	11
4.2 Tradeoffs when mapping cropped area over large geographic areas.....	12
4.3 Further considerations regarding the cropped area algorithm .....	12
<b>5. Conclusions</b> .....	<b>14</b>
<b>Figures</b> .....	<b>15</b>
<b>Tables</b> .....	<b>23</b>
<b>References</b> .....	<b>29</b>

## List of Figures

**Figure 1.** The two sites in this study are located in the states of Uttar Pradesh and Bihar in the eastern Indo-Gangetic Plains (IGP). The locations of the study sites are indicated in red. Geographic Coordinate System: WGS 1984.

**Figure 2.** Typical phenology curve for a cropped pixel at our study sites. Black points are raw 16-day NDVI composite values and the line represents smoothed values. Red points indicate relative minimum and maximum.

**Figure 3.** Typical phenology curves for three common land-cover types found at our study sites. All three classes exhibit a relative minimum followed by a relative maximum, but the amplitude and maximum NDVI value are highest for cropped pixels.

**Figure 4.** Workflow for preprocessing and analysis of MODIS, Landsat 8, Sentinel-2, and PlanetScope Imagery.

**Figure 5.** PlanetScope imagery false color composite (red=NIR, green=red, blue=green) (A) overlaid with cropped area maps produced from MODIS (B), Landsat 8 (C), Sentinel-2 (D), and PlanetScope (E) for the Uttar Pradesh site. Datum: WGS 1894. CRS: UTM Zone 44N.

**Figure 6.** PlanetScope imagery false color composite (red=NIR, green=red, blue=green) (A) overlaid with cropped area maps produced from MODIS (B), Landsat 8 (C), Sentinel-2 (D), and PlanetScope (E) for the Bihar site. Datum: WGS 1894. CRS: UTM Zone 45N.

**Figure 7.** Random forest classification of land cover at the Uttar Pradesh site. Datum: WGS 1894. CRS: UTM Zone 44N.

**Figure 8.** Random forest classification of land cover at the Bihar site. Datum: WGS 1894. CRS: UTM Zone 45N.

**Figure 9.** Sensitivity analysis of the two threshold methods used in this study, grouped by study site.

## **List of Tables**

**Table 1.** Optimal amplitude and maximum NDVI for separating cropped and fallow pixels according to CART

**Table 2.** Variables included in the random forest classification

**Table 3.** Accuracy assessment of the random forest model at the Bihar site for each class (A) and aggregate classes (B)

**Table 4.** Accuracy assessment of the random forest model at the Uttar Pradesh site for each class (A) and aggregate classes (B)

**Table 5.** Overall accuracy and Kappa values for each site, sensor, and method used in this study

**Table 6.** Overall Accuracies and Kappa values for PlanetScope imagery resampled at coarser resolutions

**Table 7.** Evaluating each sensor in terms of three criteria

# 1. Introduction

## *1.1 Background*

Accurate, fine-scale agricultural statistics are an important tool for understanding patterns of food production across the globe<sup>1-3</sup>. Such statistics are widely used by researchers and policy makers to understand agricultural responses to environmental changes, identify yield gaps, and to inform possible solutions to address growing food demand<sup>4-6</sup>. The Food and Agriculture Organization (FAO) and government censuses produce agriculture statistics for many areas, but these are often calculated at the state or national scale<sup>7</sup>. These statistics, while useful for understanding regional and global trends, may miss or obscure finer scale patterns that play an important role in food production<sup>8</sup>. This is especially true in smallholder agricultural systems, where agricultural practices and food production are often very heterogeneous across even small geographic areas<sup>9</sup>. Production of fine-scale agricultural statistics is therefore of particular importance in smallholder systems. Such statistics better inform researchers and policy makers trying to understand the factors affecting food production.

Agricultural production is generally understood as the product of cropped area and crop yield. For the purposes of this study we define cropped area as an agricultural area under active cultivation during a given year. It is distinct from land reserved for agriculture, which may or may not be active at a given time. In order to study trends in agricultural production, researchers have historically used satellite imagery to generate data at finer spatial scales than would otherwise be available<sup>10-12</sup>. Previous studies have shown that cropped area and crop yield can be mapped using multi-temporal 500 m MODIS imagery and 30 m Landsat imagery at finer spatial scales than available from the FAO or government censuses which, at their finest, aggregate data at the district level<sup>13-15</sup>. An additional benefit of cropped area maps generated with remote sensing data is that they are spatially explicit and therefore provide additional information on location and variation of cropped area within a given district. Studies have shown that satellite sensors provide sufficient accuracies for crop yield monitoring and economic applications such as commodity pricing, especially in areas dominated by relatively large or industrial agriculture practices<sup>16</sup>. Thus, much of

agricultural mapping research has been conducted in regions where cropped areas are relatively large and homogenous<sup>17-19</sup>.

However, the accuracies from analyses using these sensors may not be sufficient for use in food security applications, especially in smallholder systems<sup>20-22</sup>. Agricultural plots, defined as contiguous areas of land used for growing crops, can be heterogeneous on the landscape and quite small (<2 ha) in smallholder systems, and in some cases may be smaller than a MODIS (250 m) or even a Landsat (30 m) pixel<sup>13,23</sup>. Previous studies have demonstrated that reliable mapping of smallholder systems may require the use of imagery with higher spatial resolution than MODIS or Landsat<sup>23-25</sup>. For this reason, high or very high spatial resolution satellite sensors such as Sentinel-2 (10 m) or PlanetScope (3.7 m) may be better suited for applications in smallholder systems.

Recent advancements in remote sensing technology have led to the proliferation of high and very high resolution satellite sensors, and with them a vast increase in the quantity of geospatial data<sup>26</sup>. Sentinel-2, for example, was launched by the European Space agency in 2015 and captures global imagery every 5 days at a resolution of 10 meters. In addition, the Planet constellation of Planet Dove satellites includes more than 130 PlanetScope sensors each with a 3.7 m resolution, collectively capturing ~346,000,000 km<sup>2</sup> of imagery almost every day<sup>27</sup>. The increased spatial and temporal resolution of these sensors offer great potential as a tool for researchers studying patterns at fine spatial scales, and have the potential to significantly improve current satellite-based estimates of cropped area.

Mapping cropped area using satellite imagery presents numerous challenges. One especially difficult problem is that it is often difficult to separate fallow agricultural areas from those under active cultivation in a given year. As a result, many global products that use 500 m or 250 m MODIS data or 30 m Landsat data lump these two categories together, which may lead to biased cropped area estimates, especially in smallholder systems<sup>28</sup>. There is a need, therefore, for the development of cropped area mapping methodologies that utilize finer-scale data and are capable of distinguishing fallow from actively cropped pixels even across heterogeneous landscapes.

Recent studies have shown that very high spatial resolution sensors such as SkySat (2 m) and Worldview-2 (1.85 m) can be used to extract smallholder cropped area measurements that are more accurate than moderate and coarse spatial resolution sensors such as Landsat 8

or MODIS respectively<sup>20,24,25</sup>. Few studies, however, have examined the utility of Sentinel-2 and PlanetScope satellite sensors for such applications. Sentinel-2 offers great potential for fine-scale cropped area mapping because it is a free, globally available sensor with a higher spatial resolution than MODIS or Landsat 8, and a relatively high temporal resolution (5 days). Very high-resolution PlanetScope imagery also shows great promise for use in smallholder cropped area mapping, as it offers both high temporal (~ 3 days) and spatial (3.7 m) resolution at a lower cost than most commercial high-resolution products. Both of these sensors have the potential to improve current satellite-based estimates of cropped area.

Smallholder agriculture is found globally<sup>13,20,29</sup>. A particularly large and important global area to consider is the Indian subcontinent. India is one of the largest agricultural producers in the world where smallholder agriculture is the primary mode of production<sup>30</sup>; it is estimated that some 70% of India's rural population rely on agriculture as their primary livelihood<sup>31</sup>. Furthermore, food security in India is predicted to suffer some of the greatest negative effects from climate change in the coming decades<sup>32,33</sup>, highlighting the urgent need for accurate, fine-scale agricultural statistics in the region. The main goal of this study is, therefore, to assess cropped area estimates on smallholder farms in the eastern Indo-Gangetic Plains (IGP) region of India using MODIS (250 m), Landsat 8 (30 m), Sentinel-2 (10 m), and PlanetScope (3.7 m) satellite sensors. In particular, we examine how spatial resolution of satellite sensors affects the accuracy of the cropped area estimates in this system.

## *1.2 Study Area*

For the purposes of this study we focus on the eastern Indo-Gangetic Plains (IGP) region of India. Seasonality in this region is typically characterized in terms of two seasons: the dry winter season (rabi), which takes place from approximately November through April, the monsoon season (kharif), which occurs from June through October. In the eastern IGP farmers typically grow wheat during the winter season and rice during the monsoon season. We only focused on the winter growing season for the purposes of this study because it has less precipitation than the monsoon season and as a result it is much easier to obtain a sufficient amount of cloud free imagery.

The IGP is located in the northern part of India, south of the Himalayan mountain range. The plains are largely flat and have numerous rivers running through them. The area was once open grassland, but is now densely populated and dominated by agriculture as the

highly fertile alluvial soil of the IGP make it ideal for cultivation. India is the second largest producer of both rice and wheat globally, and the majority of this production occurs through smallholder agriculture in the IGP<sup>34</sup>.

Because of the small size of smallholder agricultural plots (typically  $\leq 2$  ha), mapping cropped area in the IGP is particularly challenging<sup>24,25,29</sup>. This provides motivation for the development of more robust methods for satellite-based cropped area mapping in this region. We focus specifically on the eastern part of the IGP because farmers in the eastern IGP tend to be more negatively affected by heat stress and tend to have lower yields and higher yield gaps than farmers in the western IGP<sup>10</sup>. Many organizations are actively working in this area to improve yields and they could benefit from more explicit cropped area estimates.

We selected agricultural areas from two states in the IGP—Bihar, and Uttar Pradesh—for analysis in this study (Figure 1). From each state, we identified a 10x10 km area that appeared to be representative of the larger region based on visual interpretation of very high-resolution imagery available from Google Earth. These areas formed our two study sites. The Uttar Pradesh site we selected is a mosaic of active and fallow agricultural plots, broken up only by developed or urban areas and roads. The Bihar site is also mostly agricultural area with some urban areas interspersed, but also has a river running through it and some areas of forest and shrub. Classified land cover maps of the two study areas can be seen in Figures 7 and 8.

## 2. Methods

### *2.1 Data acquisition and preprocessing*

Our approach comparing sensors at multiple-spatial resolutions also relied on multi-temporal imagery from these sensors so as to include the full extent of the winter growing season. Thus the imagery used in this study was collected from October 1, 2017 to April 15, 2018. For MODIS 250 m imagery, we used the 16-day NDVI composite product available on Google Earth Engine (GEE)<sup>35</sup>. Additionally, we used the 30 m Landsat 8 Tier 1 Surface reflectance (SR) and the 10 m Sentinel-2 Multispectral Instrument Level 1-C top of atmosphere (TOA) reflectance products available through GEE. The Sentinel-2 imagery was then manually corrected to surface reflectance using the Py6 method<sup>36,37</sup>. For Landsat 8 and Sentinel-2 imagery, we used the built-in cloud masking algorithms that take advantage of the QA band to remove cloudy pixels from each image. Next, we generated composite imagery that selected the highest NDVI value for a given pixel for each 16-day increment during the growing season. 3.7 m Planet imagery was downloaded using the Planet API<sup>27</sup>, and two cloud-free, high quality images per month were selected as evenly spaced as was possible. In total, this resulted in about 12 images from each sensor for each study area.

For each pixel in the multi-temporal image collections, we fit a cubic smoothing spline to the raw NDVI phenology curves in order to smooth the signal and remove any false peaks caused by noise or atmospheric effects (Figure 3). Next, we examined unique phenological characteristics for different land-cover classes in order to determine an appropriate method for distinguishing between cropped pixels and non-cropped pixels (Figure 4). Based on our analysis and similar studies using this method<sup>13,38</sup>, we determined that cropped pixels could be identified by a relatively simple algorithm that incorporates a few key parameters, which will be discussed in detail in the following section. A full workflow from this study can be seen in Figure 2.

### *2.2 Phenology based cropped area classification algorithm*

The algorithm we developed for cropped pixel classification first identifies a relative minimum followed by a relative maximum within the phenology curve (Figure 3). These points roughly correspond to the date of sowing and the peak of the growing season. The first derivative of the phenology curve is used to identify these minima and maxima within the

NDVI timeseries for each pixel, as at these locations the derivative changes sign. Pixels that exhibit a relative minimum followed by a relative maximum are identified as potentially cropped.

Relying on relative minima and maxima alone, however, is not sufficient to map cropped area in this system. This is because many areas that are not cropped, especially fallow fields, may still exhibit a relative minimum and maximum (Figure 4). It is important, then, to include within the algorithm a method to separate fallow and cropped pixels. Many phenological features, such Normalized Difference Vegetation Index (NDVI), amplitude, and rate of decrease, can be used to separate fallow and cropped pixels<sup>28,38</sup>. In this study, we evaluated the effectiveness of two methods. The first method we examined uses a maximum NDVI threshold value. This method has been applied in previous studies measuring cropped area across large spatial and temporal scales<sup>25</sup>. The second method we explored uses an NDVI amplitude threshold. The amplitude, or the difference between the relative maximum and minimum in the phenology curve, has been found to be useful for separating fallow and cropped pixels for cropped area mapping<sup>38</sup>.

In this study, each pixels that exhibit a single relative minimum followed by a relative maximum are considered to be potentially cropped (Figure 2). Next, we used the threshold values (either maximum NDVI or amplitude) in order to separate cropped from fallow pixels. In other words, pixels that exhibit multiple peaks, lack a relative minimum or relative maximum, or have an amplitude or maximum NDVI of less than the threshold value are classified as non-cropped pixels by the algorithm. For each site, we determined an optimal maximum NDVI threshold and amplitude threshold using a decision tree trained with cropped and fallow pixels for each site. We then took the average value across all sensors and sites in order to use consistent threshold values throughout our study areas (Table 1). Next, we assessed the relative accuracy of both methods individually to determine which of the two threshold methods (maximum NDVI threshold or amplitude threshold) was more reliable for our study areas. We also performed a sensitivity analysis for each threshold method to understand the how sensitive the algorithm was to changes in the threshold value (Figure 5).

After applying the algorithm to each multi-temporal dataset, our method output a classified raster layer indicating whether each pixel from a given multi-temporal NDVI

image collection was considered “cropped” or “not cropped” (Figure 5 and 6). From these raster layers we were then able to analyze the estimated cropped area from each sensor for a given study site.

### *2.3 Validation using random forest classification*

In order to validate the cropped area maps produced from our phenology-based algorithm, we generated a separate classified map using random forest classification (Figures 7 and 8). Random forests are a popular method for image classification due to the high accuracies they produce and their ability to use a large number of predictor variables without over-fitting<sup>39</sup>. Training and testing polygons were digitized for the random forest model using visual image interpretation of a composite image of maximum NDVI values between December and March generated from the PlanetScope imagery for each site. Agricultural plots that had relatively high maximum NDVI (typically  $>0.5$ ) during the growing season were considered cropped. For each site, multiple distinct land-cover classes were identified for inclusion in the model. For each land-cover class, the number of polygons digitized was roughly proportional to the area that class occupied relative to the study area.

The imagery used to predict land-cover type included four PlanetScope images with RGB and VIR bands. These four images spanned four months of the growing season, with one image included from each month. NDVI for each of these images was also calculated and included in the model. Additionally, a maximum NDVI composite from December through March was included to capture the peak of the growing season, and a minimum NDVI composite from October through December was included to capture the start of the growing season. The difference between the maximum and minimum NDVI values was also included in the model order to better distinguish between cropped and fallow pixels. Lastly, we included the JAXA 30 meter digital surface model in the random forest to help distinguish features such as urban areas, which tend to have higher elevation values on average than other land-cover classes. A full list of the variables included in the random forest, and their relevant properties, can be found in the Table 2.

We trained the random forest classifier using 70% of the digitized polygons for each site, and saved the remaining 30% for testing. For each of the land-cover classes, we randomly sampled 3000 pixels for training. Accuracy was examined both for individual land-cover classes (e.g., urban, cropped, fallow) and also at the aggregate class level of “cropped”

or “not cropped” for each site (where all non-cropped classes were labeled “not cropped”). We observed accuracies of >99% at the aggregate levels, which we determined to be sufficiently high for validating the cropped area classification algorithm (Tables 3 and 4). Once a sufficiently accurate random forest classification was developed, we selected 10,000 random pixels without replacement at each site and assessed the accuracy of the cropped area algorithm using the random forest classification as a validation map.

### 3. Results

#### *3.1 Comparison of methods for separating cropped and fallow fields*

In order to determine if one method would be more reliable for separating cropped and fallow fields, we assessed the maximum NDVI and amplitude threshold methods separately. In both cases, the optimal threshold value identified by the decision tree was slightly different depending on the sensor and site. To account for random variation and to make the methods more comparable, we took the average values across all sensors and sites and identified an optimal amplitude threshold of 0.26 and an optimal maximum NDVI threshold of 0.6 (Table 1).

Overall, the amplitude threshold and maximum NDVI threshold methods generally produced similar overall accuracies when using the optimum value selected by the decision tree (Table 5). The maximum NDVI method was slightly more accurate in the Uttar Pradesh site, while the amplitude method was slightly more accurate at the Bihar site. A sensitivity analysis of each method, however, showed that the amplitude threshold may be a more robust method for removal of fallow pixels because it produces more consistent peak accuracies across a range of values at both sites (Figure 5). For this reason, we focused mainly on the amplitude threshold method for the rest of our analysis.

#### *3.2 Cropped area map accuracy assessment*

In general, the overall accuracy of cropped area maps produced in this study increased with sensor resolution (Table 5). In order to understand the role of spatial resolution in overall accuracy, as opposed to other differences between sensors, we resampled the PlanetScope surface reflectance imagery using bilinear interpolation to resolutions that corresponded to the other sensors in this study (10 meters, 30 meters, and 250 meters). We found that the aggregated PlanetScope imagery displayed similar trends in overall accuracy when resampled at coarser resolutions, suggesting that the resolution of the sensors, more so than other sensor differences, are driving the differences in accuracy (Table 6).

#### *3.3 Evaluating sensors in terms of three criteria*

We further evaluated each sensor in terms of three criteria: data availability, accuracy, and ease of use (Table 7). Our qualitative analysis of each sensor showed that PlanetScope imagery, though highest in accuracy, scores low in ease of use because of high computational

requirements and additional preprocessing steps such as clipping, downloading, and mosaicking. Despite these challenges, the PlanetScope imagery is available at surface reflectance and so it does not have to be atmospherically corrected. The PlanetScope imagery scored moderate in terms of data availability because it is cheaper than other very high-resolution sensors, but there is a monthly quota that limits the availability of freely downloadable imagery.

The imagery from Sentinel-2 scored moderate in terms of accuracy, and was only outperformed in accuracy by the PlanetScope imagery. Because it has a five-day global repeat time and is freely available, Sentinel-2 scored high in terms of data availability. Sentinel-2 received a moderate score for ease of use only because there is not currently a surface reflectance product available across the globe. As a result, atmospheric correction must be performed on the imagery before it can be used, adding an additional step during preprocessing of Sentinel-2 imagery.

Though generally lower than Sentinel-2, Landsat 8 also scored moderate for accuracy because overall accuracies were in the range of 71-77%. Because Landsat 8 surface reflectance products are readily available, Landsat 8 scored high for ease of use. Landsat 8 scores low, however, for image availability, due to the combination of a low temporal resolution (16 days) and the high degree of cloud cover in this region. These factors result in sparse Landsat 8 imagery throughout the growing season, which can make it difficult to construct accurate NDVI phenology curves.

Lastly, MODIS scored high both in terms of image availability and ease of use. The daily coverage of the MODIS sensor allows for quality mosaicking of imagery and results in almost complete coverage throughout the growing season. Similarly, the 16-day NDVI composite product from MODIS is readily available, and can be used with very little preprocessing. In terms of accuracy, however, MODIS was the only sensor in this study to score low. Despite the advantages of MODIS in terms of image availability and ease of use, the low accuracies (in the range of 60-67%) indicate that it may not be suitable for use at fine spatial scales, especially in complex or heterogeneous landscapes with small patch sizes.

## 4. Discussion

### *4.1 The role of sensor resolution in cropped area mapping in the eastern IGP*

The results of this study add to a growing body of literature that demonstrates the importance of fine-scale agricultural statistics in smallholder systems<sup>24,25,40</sup>. Satellite-based cropped area estimates are frequently used in research and can even inform policy decisions or on-the-ground interventions<sup>10</sup>. Given the wide range of applications for which these data may be used, it is important that cropped area estimates are both accurate and relevant for the scale at which they will be used. Our results show that sensor resolution can have dramatic effects on the accuracy of cropped area estimates, especially across fine spatial scales. Overall, MODIS performed poorly in the two sites examined in this study (60-67% accuracy), and Landsat 8 performed only somewhat better (71-77% accuracy). Additionally, Sentinel-2 had consistently higher accuracies (78-82%) than Landsat 8, while PlanetScope had the highest accuracies of all the sensors used in this study (80-87%).

Given the significant influence that sensor resolution can play in accuracy of cropped area estimates, it is critical that sensors with an appropriate resolution are chosen when mapping cropped area in smallholder systems. Our results show that, in order to produce maps with even moderate accuracies, mapping should be done with sensors that have a resolution finer than the typical plot size. In the case of smallholder systems in the eastern IGP, this suggests that maps at the resolution of MODIS or even Landsat 8 may not be appropriate for understanding cropped area. More broadly, while global cropped area products can be useful for large-scale studies, such as those at the regional or global level, they may not be reliable for studying systems at finer scales or distinguishing features that are smaller than the sensor resolution. Our results indicate that this is particularly true for the cropped area mapping in the eastern IGP. Although smallholder agriculture in our study areas appears to occur in fairly cohesive patches on the landscape, it is difficult for our classification algorithm to distinguish actively cropped pixels from fallow pixels when using coarse and moderate resolution sensors. These results highlight the importance of generating cropped area maps that are specific to scale of the system in question. When mapping cropped area in the eastern IGP, our results indicate a need for fine-scale cropped area maps

at the resolution of Sentinel-2 or even PlanetScope. This may also be true for areas in other global regions where smallholder agriculture is predominant<sup>23</sup>.

#### *4.2 Tradeoffs when mapping cropped area over large geographic areas*

Despite the need for high-resolution sensors for mapping cropped area in smallholder systems, there are certain tradeoffs to consider, especially when mapping over large spatial or temporal scales. While high-resolution imagery has proliferated in recent years, it still may be difficult to acquire sufficient imagery over large spatial areas, and the computational requirements of mapping over large spatial areas increase significantly when using high-resolution imagery. As a result, moderate resolution sensors such as Landsat 8 may be more appropriate when mapping over very large areas such as continents or global mapping<sup>25</sup>. These coarser resolution sensors may also work well in agricultural systems where plot sizes are larger, such as in industrial agricultural systems. Researchers must consider the tradeoff between mapping accuracy at fine spatial scales and ease of use across large geographic areas, and should ideally choose the sensor with the highest resolution that can still be applied across the area of interest.

#### *4.3 Further considerations regarding the cropped area algorithm*

Beyond considerations of sensor resolution and accuracy, there are other factors that should inform methodology when mapping cropped area. In this study, we used relative minima, relative maxima, and amplitude from the phenology curve of a single growing season to map cropped area. We were able to develop an algorithm to identify cropped areas using these features based on our prior knowledge of phenological patterns in this system. Even still, the selection of an optimal amplitude threshold varied somewhat by site. Though less involved than gathering training data for a supervised classification, we still had to determine an optimal amplitude threshold to separate fallow from cropped pixels for each site. Variability in this optimal value could play an important role in mapping accuracy, and further studies will be needed to determine if there is a single optimal value for all of the eastern IGP, or if the amplitude threshold should be calculated from training data at even finer scales.

The variability in the optimal amplitude threshold also points to additional questions about the application of this automated method in other study areas outside of the eastern IGP. Climate, ecosystem type, agricultural practices, and many other factors influence

phenology, leading to a great diversity of crop phenological patterns around the world. It would not be appropriate then, to apply this method to another region without first understanding the phenology of each land-cover type in the region. Studies mapping cropped area in western Niger, for example, found that fallow areas typically have higher amplitude than cropped areas, the opposite of what we observe in the eastern IGP<sup>38</sup>. Similarly, a study in Europe found fallow areas to exhibit a smooth, bell shaped NDVI phenology profile, while active farmland was characterized by more irregular NDVI temporal profiles with one or more narrow peaks<sup>41</sup>. These examples highlight the importance of a knowledge-based approach to cropped area mapping that takes into consideration the unique features of the system in question.

## 5. Conclusions

We observed that the overall accuracy of cropped area maps increased when using higher resolution sensors. In particular, we found that the accuracy of cropped area estimates can be greatly improved by selecting a sensor with a resolution smaller in size than a typical agricultural plot (<2 ha). MODIS was found to be inaccurate in smallholder systems in the eastern IGP, and cropped area mapping at the resolution of MODIS may not be appropriate for mapping cropped area in this system. Landsat 8, though better than MODIS, exhibited only moderate accuracies and was limited by its temporal resolution. Sentinel-2 showed great promise for applications in smallholder systems given its relatively high temporal frequency and fine spatial resolution, and PlanetScope produced the most accurate cropped area maps but requires more preprocessing than other sensors.

In conclusion, we find that the semi-automated method presented in this study can be an effective tool for mapping cropped area in the eastern IGP, and it offers some key benefits over other methods. First, it requires less training data than other image classification techniques such as random forest classification. Another benefit of this method is that it can discriminate between cropped and fallow pixels. Many global cropped area products do not separate cropped and fallow pixels, often resulting in an overestimation of active cropped area<sup>28</sup>. In future studies we will apply this method to other sites in the IGP, eventually scaling up to the district level to compare our crop area estimates with census data. This method also has potential for application in other areas, though the phenological profiles of all land-cover types must be well understood before this method can be applied in any novel system.

## Figures

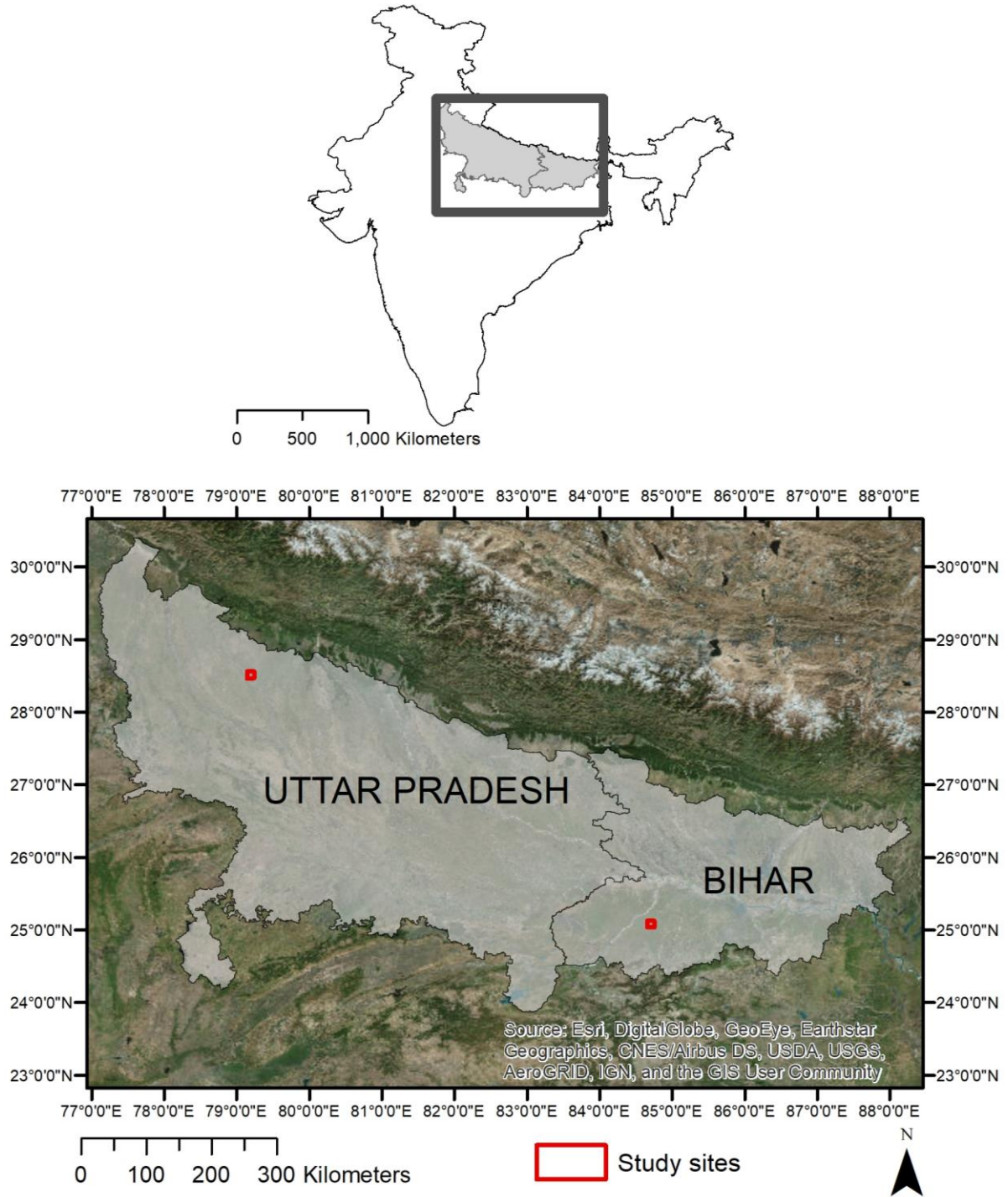


**Figure 1.** The two sites in this study are located in the states of Uttar Pradesh and Bihar in the eastern Indo-Gangetic Plains (IGP). The locations of the study sites are indicated in red. Geographic Coordinate System: WGS 1984.

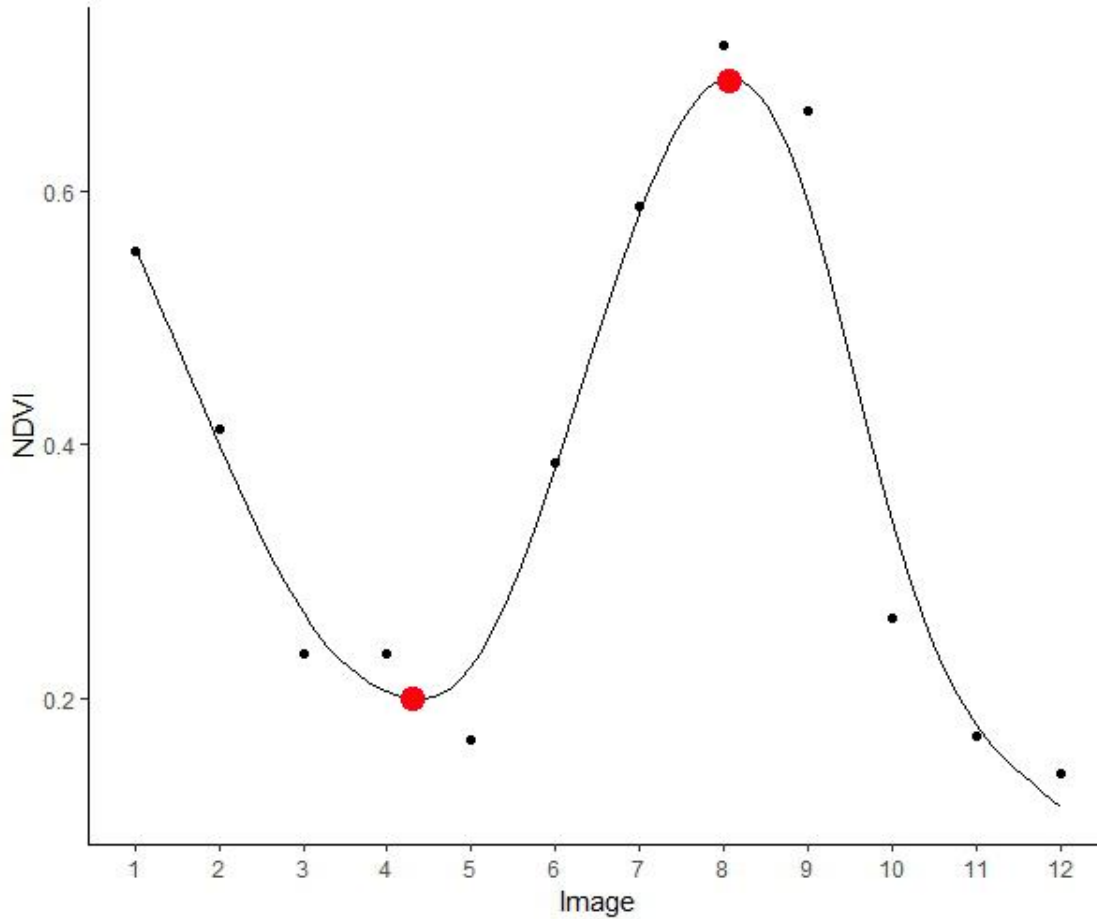


**Figure 2.** Typical phenology curve for a cropped pixel at our study sites. Black points are raw 16-day NDVI composite values and the line represents smoothed values. Red points indicate relative minimum and maximum.

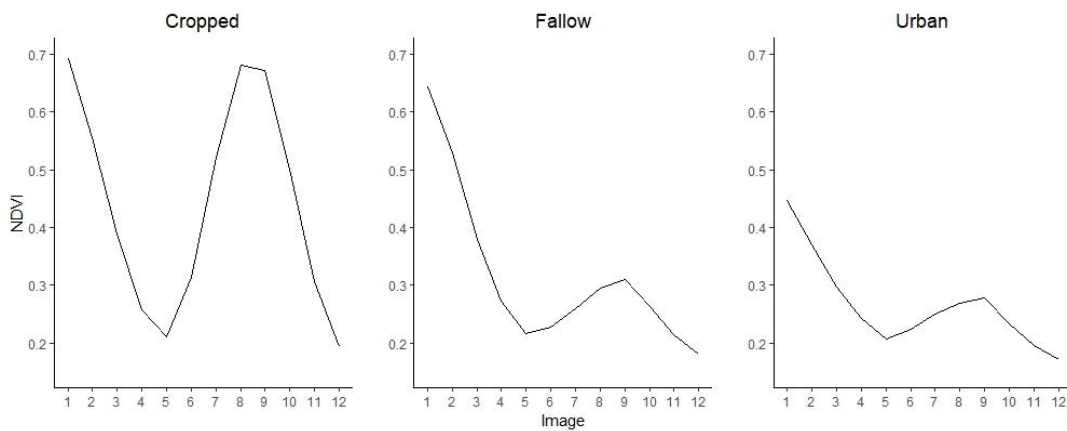


**Figure 3.** Typical phenology curves for three common land-cover types found at our study sites. All three classes exhibit a relative minimum followed by a relative maximum, but the amplitude and maximum NDVI value are highest for cropped pixels.

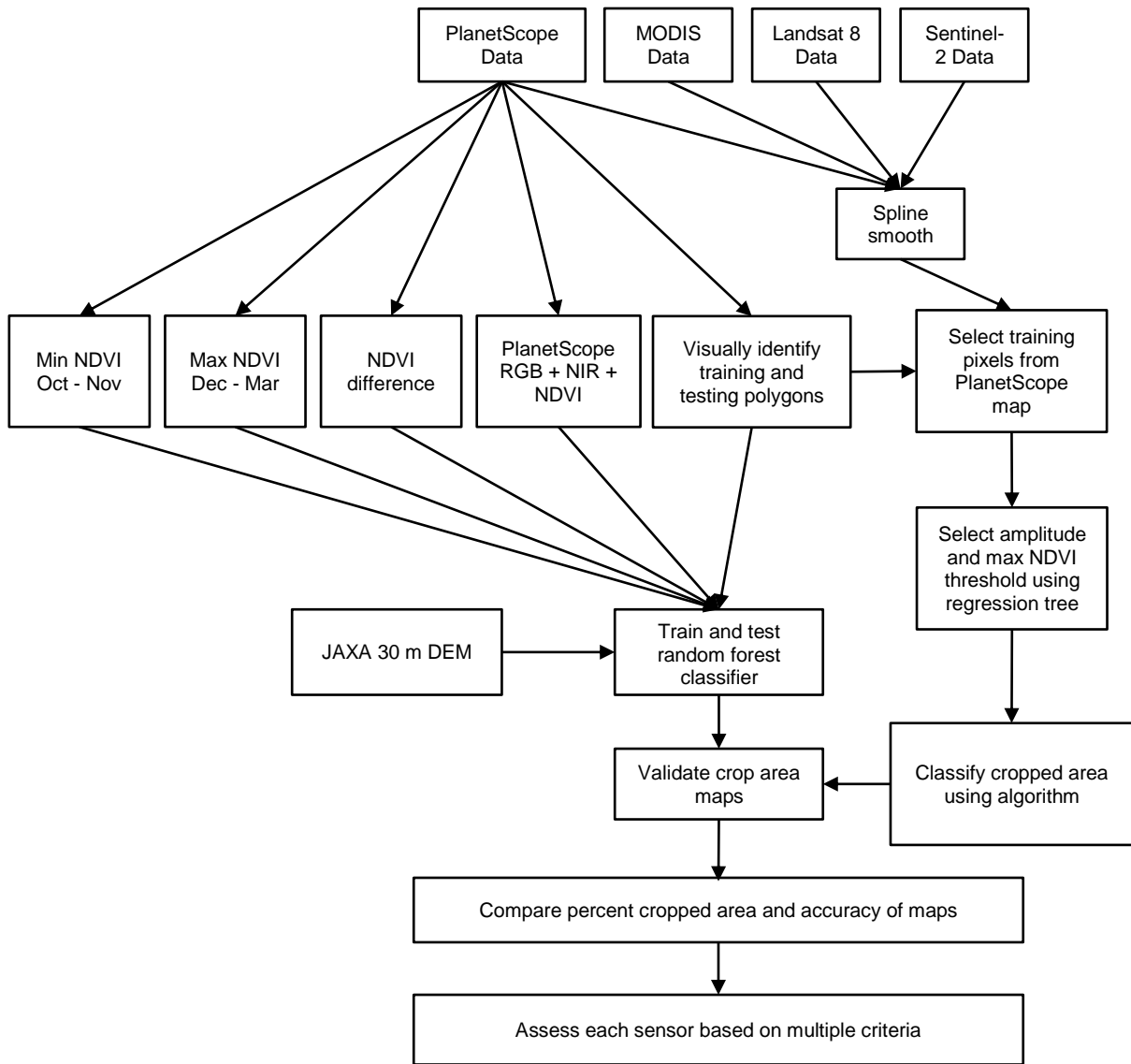


**Figure 4.** Workflow for preprocessing and analysis of MODIS, Landsat 8, Sentinel-2, and PlanetScope Imagery.

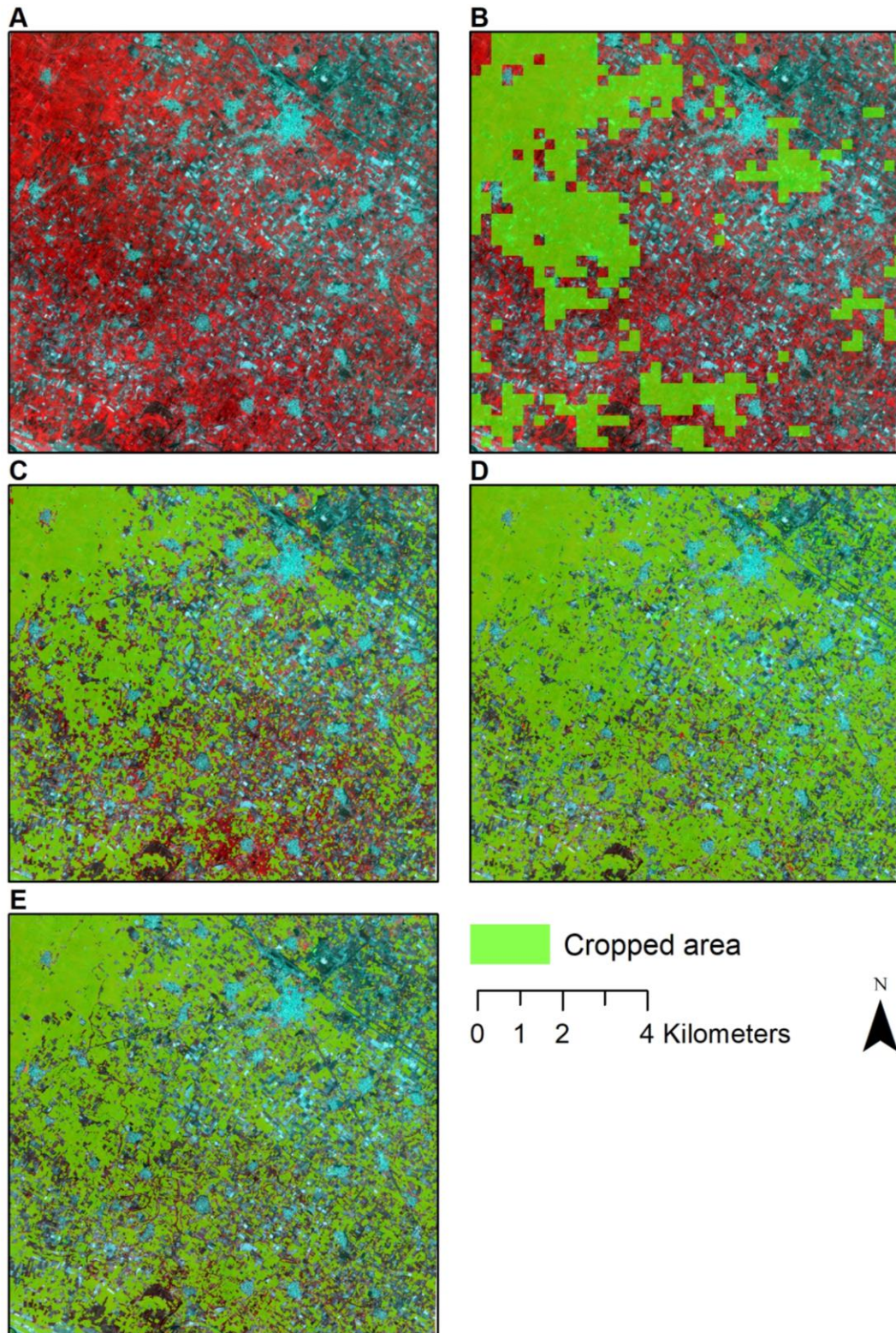


**Figure 5.** PlanetScope imagery false color composite (red=NIR, green=red, blue=green) (A) overlaid with cropped area maps produced from MODIS (B), Landsat 8 (C), Sentinel-2 (D), and PlanetScope (E) for the Uttar Pradesh site. Datum: WGS 1894. CRS: UTM Zone 44N.

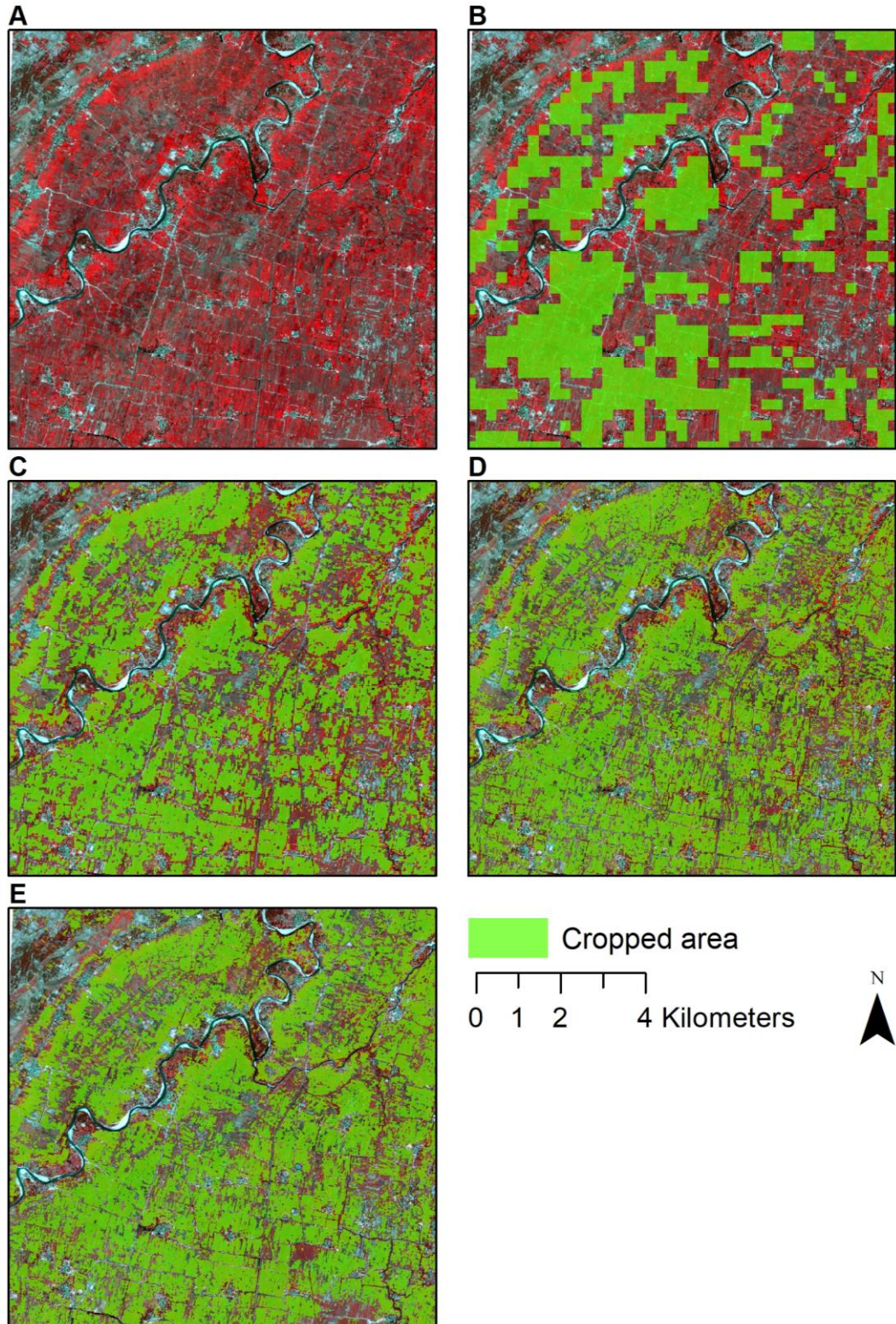


**Figure 6.** PlanetScope imagery false color composite (red=NIR, green=red, blue=green) (A) overlaid with cropped area maps produced from MODIS (B), Landsat 8 (C), Sentinel-2 (D), and PlanetScope (E) for the Bihar site. Datum: WGS 1894. CRS: UTM Zone 45N.

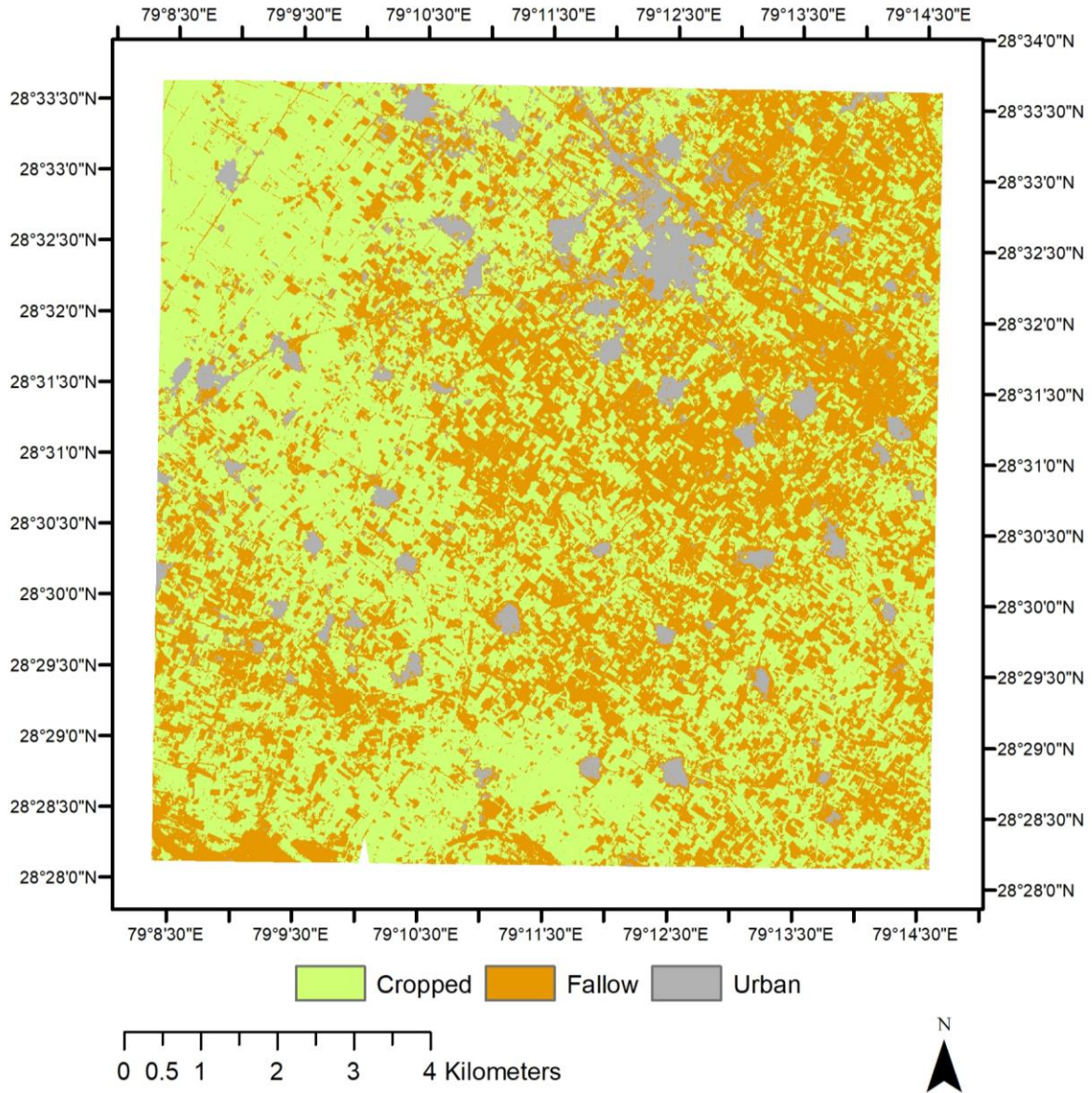


**Figure 7.** Random forest classification of land cover at the Uttar Pradesh site. Datum: WGS 1894. CRS: UTM Zone 44N.

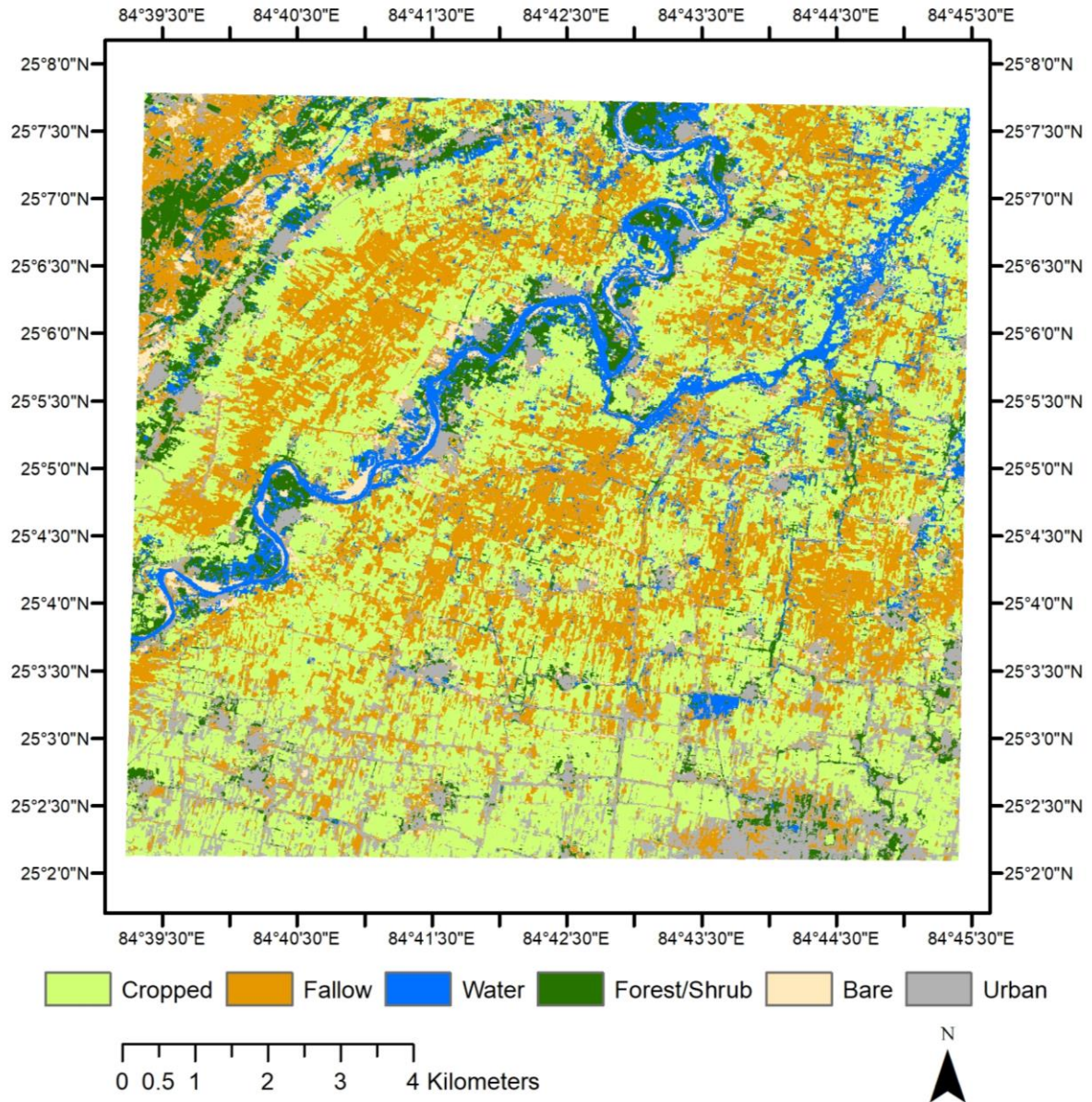


**Figure 8.** Random forest classification of land cover at the Bihar site. Datum: WGS 1894.  
CRS: UTM Zone 45N.

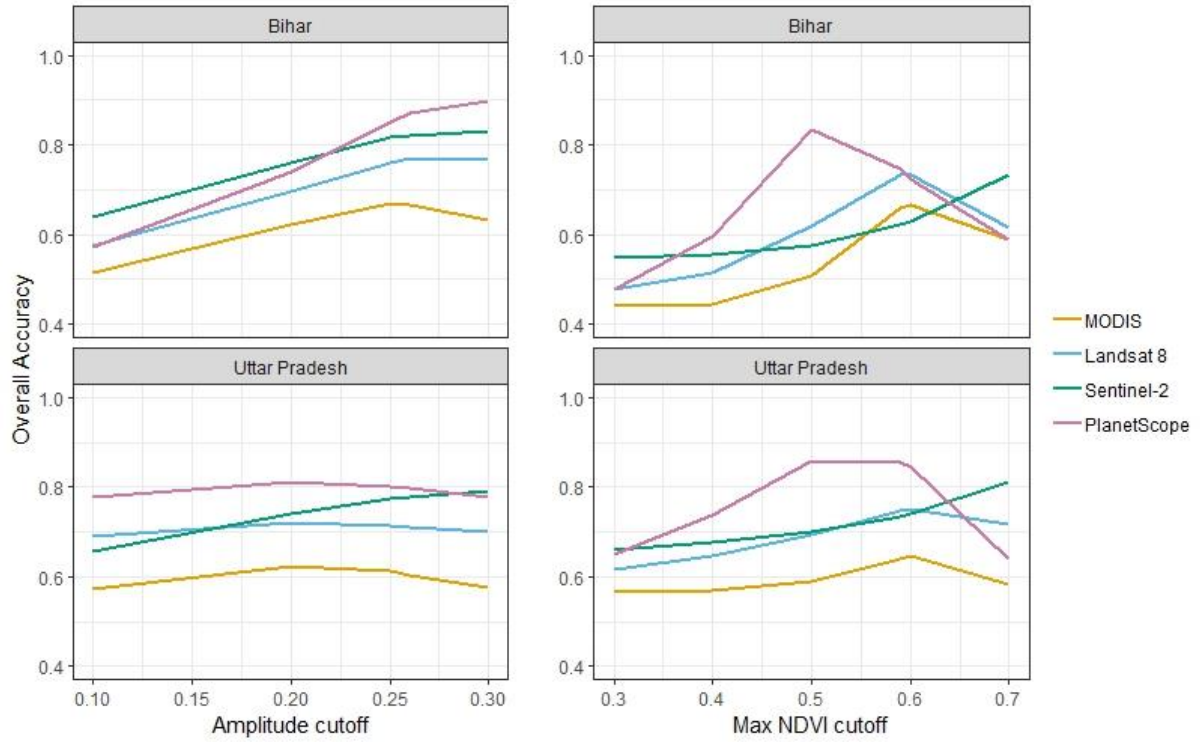


**Figure 9.** Sensitivity analysis of the two threshold methods used in this study, grouped by study site.

## Tables

**Table 1.** Optimal amplitude and maximum NDVI for separating cropped and fallow pixels according to CART

<b>Sensor</b>	<b>Site</b>	<b>Amplitude threshold</b>	<b>Maximum NDVI threshold</b>
MODIS	Uttar Pradesh	0.26	0.6
Landsat	Uttar Pradesh	0.28	0.6
Sentinel	Uttar Pradesh	0.33	0.71
Planet	Uttar Pradesh	0.23	0.52
MODIS	Bihar	0.28	0.57
Landsat	Bihar	0.25	0.54
Sentinel	Bihar	0.23	0.78
Planet	Bihar	0.2	0.47
<b>Mean value</b>		<b>0.26</b>	<b>0.60</b>

**Table 2.** Variables included in the random forest classification

<b>Variable Name</b>	<b>Source</b>	<b>Imagery date</b>	<b>Resolution</b>	<b>Description</b>
Minimum NDVI	Derived from PlanetScope	October 2017 - November 2017	3.7 meters	Minimum NDVI value from start of growing season
Maximum NDVI	Derived from PlanetScope	December 2017 - March 2018	3.7 meters	Maximum NDVI value from peak of growing season
NDVI Amplitude	Derived from PlanetScope	October 2017 - March 2018	3.7 meters	Amplitude of NDVI phenology curve.
December SR image	PlanetScope	December 2017	3.7 meters	Red, Green, Blue, NIR
December NDVI	Derived from PlanetScope	December 2017	3.7 meters	NDVI calculated from an image in December
January SR Image	PlanetScope	January 2018	3.7 meters	Red, Green, Blue, NIR
January NDVI	Derived from PlanetScope	January 2018	3.7 meters	NDVI calculated from an image in January
February SR Image	PlanetScope	February 2018	3.7 meters	Red, Green, Blue, NIR
February NDVI	Derived from PlanetScope	February 2018	3.7 meters	NDVI calculated from an image in February
March SR Image	PlanetScope	March 2018	3.7 meters	Red, Green, Blue, NIR
March NDVI	Derived from PlanetScope	March 2018	3.7 meters	NDVI calculated from an image in March
Digital Surface Model	Advanced Land Observing Satellite	January 2006 - May 2011	30 meters	The AVE (Average) band from the DSM provided by JAXA

**Table 3.** Accuracy assessment of the random forest model at the Bihar site for each class (A) and aggregate classes (B)

**A**

Actual Classified	Cropped	Fallow	Water	Forest/ shrub	Bare	Urban	User's Accuracy
Cropped	910	0	0	0	0	0	1.000
Fallow	1	562	0	0	0	84	0.869
Water	5	5	121	7	0	2	0.864
Forest/shrub	2	0	0	422	0	0	0.995
Bare	0	18	0	0	196	15	0.856
Urban	0	83	0	0	0	567	0.872
Producer's Accuracy	0.991	0.841	1.000	0.984	1.000	0.849	0.926

**B**

Actual Classified	Cropped	Not cropped	User's Accuracy
Cropped	910	0	1
Not cropped	8	2082	0.996
Producer's Accuracy	0.991	1.000	0.997

**Table 4.** Accuracy assessment of the random forest model at the Uttar Pradesh site for each class (A) and aggregate classes (B)

**A**

Actual Classified	Cropped	Fallow	Urban	User's Accuracy
Cropped	1289	0	0	1
Fallow	0	1000	67	0.937
Urban	0	39	605	0.939
Producer's Accuracy	1	0.962	0.900	0.965

**B**

Actual Classified	Cropped	Not cropped	User's Accuracy
Cropped	1289	0	1
Not cropped	0	1711	1
Producer's Accuracy	1	1	1

**Table 5.** Overall accuracy and Kappa values for each site, sensor, and method used in this study

<b>Site</b>	<b>Sensor</b>	<b>Method</b>	<b>Overall accuracy</b>	<b>Kappa value</b>
Bihar	MODIS	Amplitude	0.67	0.29
		Maximum	0.67	0.31
	Landsat 8	Amplitude	0.77	0.53
		Maximum	0.73	0.44
	Sentinel-2	Amplitude	0.82	0.64
		Maximum	0.63	0.31
	PlanetScope	Amplitude	0.87	0.74
		Maximum	0.72	0.37
Uttar Pradesh	MODIS	Amplitude	0.60	0.23
		Maximum	0.65	0.29
	Landsat 8	Amplitude	0.71	0.43
		Maximum	0.75	0.50
	Sentinel-2	Amplitude	0.78	0.55
		Maximum	0.74	0.47
	PlanetScope	Amplitude	0.80	0.60
		Maximum	0.85	0.69

**Table 6.** Overall Accuracies and Kappa values for PlanetScope imagery resampled at coarser resolutions

<b>Site</b>	<b>Resolution</b>	<b>Overall Accuracy</b>	<b>Kappa</b>
Bihar	250 m	0.69	0.36
Bihar	30 m	0.82	0.64
Bihar	10 m	0.86	0.72
Uttar Pradesh	250 m	0.63	0.28
Uttar Pradesh	30 m	0.77	0.54
Uttar Pradesh	10 m	0.79	0.59

**Table 7.** Evaluating each sensor in terms of three criteria

<b>Sensor</b>	<b>Data availability Rank</b>	<b>Ease of Use Rank</b>	<b>Accuracy Rank</b>	<b>Overall Accuracy</b>
MODIS	High	High	Low	60-67%
Landsat 8	Low	High	Moderate	71-77%
Sentinel-2	High	Moderate	Moderate	78-82%
PlanetScope	Moderate	Low	High	80-87%

## References

1. DeFries, R. *et al.* Synergies and trade-offs for sustainable agriculture: Nutritional yields and climate-resilience for cereal crops in Central India. *Glob. Food Sec.* **11**, 44–53 (2016).
2. Ray, D. K., Mueller, N. D., West, P. C. & Foley, J. A. Yield Trends Are Insufficient to Double Global Crop Production by 2050. *PLoS One* **8**, (2013).
3. Lobell, D. B., Schlenker, W. & Costa-Roberts, J. Climate trends and global crop production since 1980. *Science (80-. )*. **333**, 616–620 (2011).
4. Lobell, D. B., Sibley, A. & Ivan Ortiz-Monasterio, J. Extreme heat effects on wheat senescence in India. *Nat. Clim. Chang.* **2**, 186–189 (2012).
5. Lobell, D. B. The use of satellite data for crop yield gap analysis. *F. Crop. Res.* **143**, 56–64 (2013).
6. Godfray, H. C. J. *et al.* Food security: the challenge of feeding 9 billion people. *Science (80-. )*. **327**, 812–8 (2010).
7. Ray, D. K., Ramankutty, N., Mueller, N. D., West, P. C. & Foley, J. A. Recent patterns of crop yield growth and stagnation. *Nat. Commun.* **3**, 1293–1297 (2012).
8. Thornton, P. K., Jones, P. G., Alagarwamy, G. & Andresen, J. Spatial variation of crop yield response to climate change in East Africa. *Glob. Environ. Chang.* **19**, 54–65 (2009).
9. Jain, M., Naeem, S., Orlove, B., Modi, V. & DeFries, R. S. Understanding the causes and consequences of differential decision-making in adaptation research: Adapting to a delayed monsoon onset in Gujarat, India. *Glob. Environ. Chang.* **31**, 98–109 (2015).
10. Jain, M. *et al.* Using satellite data to identify the causes of and potential solutions for yield gaps in India's Wheat Belt. *Environ. Res. Lett.* **12**, 094011 (2017).
11. Doraiswamy, P. C., Moulin, S., Cook, P. W. & Stern, A. Crop Yield Assessment from Remote Sensing. *Photogramm. Eng. Remote Sens.* **69**, 665–674 (2013).
12. Tsiligrides, T. A. Remote sensing as a tool for agricultural statistics: A case study of area frame sampling methodology in Hellas. *Comput. Electron. Agric.* **20**, 45–77 (1998).
13. Jain, M., Mondal, P., Galford, G. L., Fiske, G. & DeFries, R. S. An automated approach to map winter cropped area of smallholder farms across large scales using

- MODIS imagery. *Remote Sens.* **9**, (2017).
14. Biradar, C. M. & Xiao, X. Quantifying the area and spatial distribution of double- and triple-cropping croplands in India with multi-temporal MODIS imagery in 2005. *Int. J. Remote Sens.* **32**, 367–386 (2011).
  15. Sakamoto, T. *et al.* A crop phenology detection method using time-series MODIS data. *Remote Sens. Environ.* **96**, 366–374 (2005).
  16. Boryan, C., Yang, Z., Mueller, R. & Craig, M. Monitoring US agriculture: The US department of agriculture, national agricultural statistics service, cropland data layer program. *Geocarto Int.* **26**, 341–358 (2011).
  17. Doraiswamy, P. C. *et al.* Application of MODIS derived parameters for regional crop yield assessment. *Remote Sens. Environ.* **97**, 192–202 (2005).
  18. Wardlow, B. D. & Egbert, S. L. Large-area crop mapping using time-series MODIS 250 m NDVI data: An assessment for the U.S. Central Great Plains. *Remote Sens. Environ.* **112**, 1096–1116 (2008).
  19. Gumma, M. K., Thenkabail, P. S., Maunahan, A., Islam, S. & Nelson, A. Mapping seasonal rice cropland extent and area in the high cropping intensity environment of Bangladesh using MODIS 500m data for the year 2010. *ISPRS J. Photogramm. Remote Sens.* **91**, 98–113 (2014).
  20. McCarty, J. L., Neigh, C. S. R., Carroll, M. L. & Wooten, M. R. Extracting smallholder cropped area in Tigray, Ethiopia with wall-to-wall sub-meter WorldView and moderate resolution Landsat 8 imagery. *Remote Sens. Environ.* **202**, 142–151 (2017).
  21. Lobell, D. B., Thau, D., Seifert, C., Engle, E. & Little, B. A scalable satellite-based crop yield mapper. *Remote Sens. Environ.* **164**, 324–333 (2015).
  22. Fritz, S. *et al.* The need for improved maps of global Cropland. *Eos (Washington, DC)*. **94**, 31–32 (2013).
  23. Cordero-Sancho, S. & Bergen, K. M. Relationships of Agricultural Land Use to an Expanded Road Network within Tropical Forest Landscapes of Cameroon and Republic of the Congo. *Prof. Geogr.* **70**, 60–72 (2018).
  24. Jain, M. *et al.* Mapping Smallholder Wheat Yields and Sowing Dates Using Micro-Satellite Data. *Remote Sens.* **8**, 860 (2016).

25. Jain, M., Mondal, P., DeFries, R. S., Small, C. & Galford, G. L. Mapping cropping intensity of smallholder farms: A comparison of methods using multiple sensors. *Remote Sens. Environ.* **134**, 210–223 (2013).
26. Ma, Y. *et al.* Remote sensing big data computing: Challenges and opportunities. *Futur. Gener. Comput. Syst.* **51**, 47–60 (2015).
27. Planet Team. Planet Application Program Interface: In Space for Life on Earth. (2017).
28. Bégué, A. *et al.* Remote sensing and cropping practices: A review. *Remote Sens.* **10**, 1–32 (2018).
29. Morton, J. F. The impact of climate change on smallholder and subsistence agriculture. (2007).
30. Chand, R., Prasanna, P. a L., Singh, A., Weekly, P. & Weekly, P. Farm Size and Productivity : Understanding the Strengths of Smallholders and Improving Their Livelihoods between. *Econ. Polit. Wkly.* **46**, 5–11 (2018).
31. Erenstein, O. & Thorpe, W. Livelihoods and agro-ecological gradients: A meso-level analysis in the Indo-Gangetic Plains, India. *Agric. Syst.* **104**, 42–53 (2011).
32. Lobell, D. B. *et al.* Prioritizing climate change adaptation needs for food security in 2030. *Science (80-. )*. **319**, 607–610 (2008).
33. Mall, R. K., Singh, R., Gupta, A., Srinivasan, G. & Rathore, L. S. Impact of climate change on Indian agriculture: A review. *Climatic Change* **78**, 445–478 (2006).
34. FAO. FAOSTAT Database on Agriculture. *Food and Agriculture Organization of the United Nations* (2017). Available at: <http://www.fao.org/faostat/>. (Accessed: 21st April 2019)
35. Gorelick, N. *et al.* Google Earth Engine: Planetary-scale geospatial analysis for everyone. *Remote Sens. Environ.* **202**, 18–27 (2017).
36. Sam Murphey. Github Repository of Sam Murphy. (2017). Available at: <https://github.com/samsammurphy>. (Accessed: 19th April 2018)
37. Wilson, R. T. Py6S: A Python interface to the 6S radiative transfer model. *Comput. Geosci.* **51**, 166–171 (2013).
38. Tong, X. *et al.* Revisiting the coupling between NDVI trends and cropland changes in the Sahel drylands: A case study in western Niger. *Remote Sens. Environ.* **191**, 286–

- 296 (2017).
39. Belgiu, M. & Drăguț, L. Random forest in remote sensing: A review of applications and future directions. *ISPRS J. Photogramm. Remote Sens.* **114**, 24–31 (2016).
  40. Mccarty, J. L. *et al.* Extracting smallholder cropped area in Tigray, Ethiopia with wall-to-wall sub-meter WorldView and moderate resolution Landsat 8 imagery. *Remote Sens. Environ.* **202**, 142–151 (2017).
  41. Estel, S. *et al.* Mapping farmland abandonment and recultivation across Europe using MODIS NDVI time series. *Remote Sens. Environ.* **163**, 312–325 (2015).